Optimizing Superconductivity: From Cuprates via Nickelates to Palladates

Motoharu Kitatani[ORCID],[1,2] Liang Si[ORCID],[3,4] Paul Worm[ORCID],[4] Jan M. Tomczak[ORCID],[4,5] Ryotaro Arita[ORCID],[2,6] and Karsten Held[ORCID][4]

[1]*Department of Material Science, University of Hyogo, Ako, Hyogo 678-1297, Japan*
[2]*RIKEN Center for Emergent Matter Sciences (CEMS), Wako, Saitama 351-0198, Japan*
[3]*School of Physics, Northwest University, Xi'an 710127, China*
[4]*Institute of Solid State Physics, TU Wien, 1040 Vienna, Austria*
[5]*Department of Physics, King's College London, Strand, London WC2R 2LS, United Kingdom*
[6]*Research Center for Advanced Science and Technology, University of Tokyo 4-6-1, Komaba, Meguro-ku, Tokyo 153-8904, Japan*

Motivated by cuprate and nickelate superconductors, we perform a comprehensive study of the superconducting instability in the single-band Hubbard model. We calculate the spectrum and superconducting transition temperature T_c as a function of filling and Coulomb interaction for a range of hopping parameters, using the dynamical vertex approximation. We find the sweet spot for high T_c to be at intermediate coupling, moderate Fermi surface warping, and low hole doping. Combining these results with first principles calculations, neither nickelates nor cuprates are close to this optimum within the single-band description. Instead, we identify some palladates, notably $RbSr_2PdO_3$ and $A'_2PdO_2Cl_2$ ($A' = Ba_{0.5}La_{0.5}$), to be virtually optimal, while others, such as $NdPdO_2$, are too weakly correlated.

Introduction.—Ever since the discovery of cuprate superconductivity [1], the material dependence of the transition temperature T_c and exploring routes toward optimizing T_c are a central quest of condensed matter physics. The recently discovered nickelate superconductors provide a new perspective to this quest. Similar to cuprates, superconductivity in nickelates emerges from a doped $3d^{9-\delta}$ ($\delta \sim 0.2$) electronic configuration of the transition metal. Besides the initial infinite-layer superconductor $Nd_{1-x}Sr_xNiO_2$ [2–8], substituting neodymium with another lanthanoid [9–11] and also the quintuple-layer compound [12] show superconductivity. This indicates that, akin to cuprates, there is a whole family of nickelate superconductors.

As for the theoretical modeling, the one-band Hubbard model is arguably the simplest effective model for cuprates [13,14]. Its tight-binding parameters can be obtained from *ab initio* calculations, and the relation between model parameters and the experimental T_c has been analyzed [15–27]. For nickelates, a similar scenario (1) with a one-band Hubbard model plus largely decoupled electron pockets has been put forward [28–35]. Based on the same density functional theory (DFT) and dynamical mean-field theory (DMFT) Fermi surface with Ni $3d_{x^2-y^2}$ orbital plus electron pockets around A and Γ momentum, a second group of scenarios (2) [36–39] emphasizes the role of holes in the Ni $3d_{z^2}$ orbital. These originate from an admixture around the Γ pocket that is predominately Nd $5d_{z^2}$. In scenario (1) this is argued to be not of primary importance for superconductivity because of the strong doping and rare earth cation dependence of the Γ pocket [3,40–42]. Finally, scenario (3) proposes an *additional* Ni $3d_{z^2}$ Fermi surface

based on self-interaction corrected (sic) DFT + DMFT [32,43–46]. Such an additional Fermi surface is also obtained in antiferromagnetically ordered DFT [47,48], GW + DMFT [49], and DFT + DMFT in the overdoped region [28,50].

While the relevant low energy model for nickelates is still under debate, a boost for scenario (1) was its successful prediction of the superconducting phase diagram [28] prior to experiments [5,6] and with high accuracy in the light of new, defect-free films [53]. Also some other experiments including, among others, the Hall coefficient, resonant x-ray spectroscopy [54], and magnetotransport [55], point toward this scenario. As for the microscopic origin of high-T_c superconductivity: while spin fluctuations mediate superconductivity in Ref. [28], the topic remains highly controversial; many different mechanisms have been proposed [56–59].

The aim of the present Letter is hence twofold: First, we would like to identify the optimal conditions for superconductivity in the Hubbard model building upon recent progress made with diagrammatic extensions of DMFT [60]. In particular, we will employ the dynamical vertex approximation (DΓA) [61], which accurately describes antiferromagnetic spin fluctuations in the parameter range where numerical quantum Monte Carlo simulations are still available [62]. Second, from a materials point of view we would like to identify cuprate- or nickelatelike materials that promise even higher T_c's. One important factor is the interaction strength U and its ratio to the hopping U/t. On a qualitative level it has been recently found [28,63] that the interaction strength is too large in nickelates. Higher T_c's
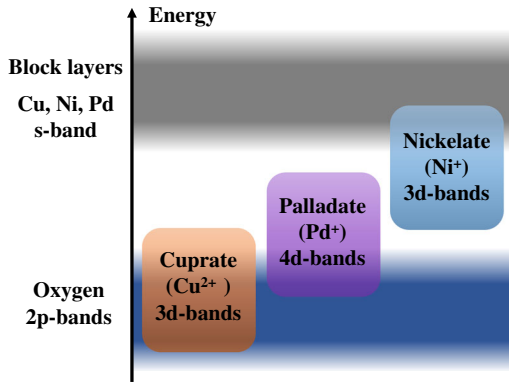
FIG. 1. Schematic picture of the energy levels for copper (Cu^{2+}), nickel (Ni^+), palladium (Pd^+) superconductors.

should thus be possible using compressive strain or pressure [64], confirmed experimentally by a record $T_c > 30$ K for nickelates under a pressure of 12 GPa with no saturation yet discernible [65]. Much more dramatic changes of U/t are possible when going from $3d$ to $4d$ transition metal oxides, which can be achieved by replacing Ni with Pd [28,33,66,67]. Here, we study this possibility on a quantitative level. We show that a one-band description is justified for palladates, and make a prediction of the superconducting phase diagram which can be tested in experiment.

Let us start by sketching the electronic structures of the above-mentioned materials schematically in Fig. 1. As is well known, the parent cuprate compounds are charge transfer insulators [68]; Cu-$3d$ and O-$2p$ bands exist at a similar energy level and are strongly hybridized. Thus the Hubbard model is justified only as an effective model that mimics the physics of the Zhang-Rice singlet [14]. In contrast, the Ni $3d$ orbital is higher up in energy by ~1 eV. The increased distance to the oxygen orbitals then makes the single-$d_{x^2-y^2}$-orbital description more suitable than for the CuO$_2$ layers in cuprates. However, DFT calculations [63,67,69–74] show that the Ni-d bands of NdNiO$_2$ now partially overlap instead with the bands of Nd in between the NiO$_2$ layers, forming the already mentioned pockets around the A and Γ momentum.

If we replace Ni ($3d$) with Pd ($4d$), the Pd $4d$ orbitals are shifted back down by ~1 eV due to the higher ionization energy of Pd compared to Ni. This removes the pockets present in the nickelates and leads to a larger d-p hybridization and minor overlap with the oxygen bands. However, we do not yet have a charge transfer state as in the cuprates. Indeed, our DFT and DMFT computations (shown in the Supplemental Material (SM) [75], Sections I–III) of the crystal and electronic structures of the nickelate NdNiO$_2$ and the palladates NdPdO$_2$, RbSr$_2$PdO$_3$, and A'_2PdO$_2$Cl$_2$ show that palladate compounds are somewhere in between cuprates and nickelates—with a single-band $d_{x^2-y^2}$ Fermi surface justifying a modeling by a single-orbital Hubbard model. Tuning the dispersion and interaction strength in palladates thus opens

so-far untapped possibilities for finding new superconductors with possibly higher T_c's.

Model and method.—We study the two-dimensional Hubbard model on the square lattice with Hamiltonian

$$\mathcal{H} = \sum_{\mathbf{k},\sigma}\epsilon_{\mathbf{k}} c^{\dagger}_{\mathbf{k},\sigma} c_{\mathbf{k},\sigma} + U\sum_{i} n_{i,\uparrow} n_{i,\downarrow}, \quad (1)$$

where $c^{\dagger}_{\mathbf{k},\sigma}(c_{\mathbf{k},\sigma})$ is the creation (annihilation) operator,

$$\epsilon_{\mathbf{k}} = -2t[\cos(k_x) + \cos(k_y)] - 4t'\cos(k_x)\cos(k_y)$$
$$- 2t''[\cos(2k_x) + \cos(2k_y)], \quad (2)$$

the energy-momentum dispersion, U the onsite Coulomb repulsion, and t, t', t'' are the nearest, second nearest, and third nearest hoppings, respectively. The model parameters are obtained from DFT, using WIEN2K [98] with the PBE [99,100] exchange correlation functional and WIEN2WANNIER [101] for projecting onto a maximally localized $3d_{x^2-y^2}$ Wannier orbital [102]. Supplemental Material Sections VI, VII, VIII, and IX provide details on the Wannier projection, the DFT calculation of A'_2PdO$_2$Cl$_2$, the stability against structural distortions, and the antiferromagnetic DFT solution, respectively. Before constructing the single-orbital model for palladates, we performed multiorbital DMFT calculations which confirm the single orbital nature of the system, see SM [75] Sec. III. The constrained random phase approximation (cRPA) is employed to estimate U. Following the previous research [28], we employed slightly enhanced values (+0.35 eV [103]) from our cRPA calculation for entangled bands [104]: 2.85 eV for NdNiO$_2$, 2.55 eV for RbSr$_2$PdO$_2$, and 2.97 eV for A'_2PdO$_2$Cl$_2$ (which are consistent with the preceding study [67]; please note that small changes in the interaction strength U do not change our conclusions). Table I provides a summary of the DFT and cRPA derived parameters [105] (for details see SM [75] Section II), which are used in subsequent DΓA calculations. Besides these material-specific Hubbard models we also include the simplest case with nearest-neighbor hopping only ($t' = t'' = 0$).

TABLE I. Summary of the DFT-derived parameters for the single-band Hubbard model, as an effective low-energy model for the nickelate NdNiO$_2$, the palladates NdPdO$_2$, RbSr$_2$PdO$_3$, and A'_2PdO$_2$Cl$_2$.

	$|t|$ (meV)	t'/t	t''/t	U_{eff}/t
NdNiO$_2$	395	−0.25	0.12	8
NdNiO$_2$ (strained)	419	−0.23	0.12	7.0–7.5
NdPdO$_2$	558	−0.17	0.13	4.5
RbSr$_2$PdO$_3$	495	−0.24	0.16	6
A'_2PdO$_2$Cl$_2$	443	−0.22	0.14	7.5
A'_2PdO$_2$Cl$_2$ (−1.5% strain)	470	−0.22	0.14	7.0
A'_2PdO$_2$Cl$_2$ (−3.0% strain)	497	−0.22	0.14	6.0

We analyze these single-orbital models by means of the DΓA [61,106–108], a diagrammatic extension of DMFT [109–111]. Similar techniques have been previously applied to unconventional superconductivity on the square lattice [112–119]. We mainly use the continuous-time quantum Monte Carlo solver from W2DYNAMICS [120] as DMFT solver, see SM [75] for details. DΓA simultaneously includes strong correlations and long-range spatial (charge and spin) fluctuations. Both are essential for modeling superconductivity in correlated electron systems. Most importantly, DΓA can describe dynamical screening effects which are crucial for accurately determining T_c [121]. It has predicted the superconducting dome in nickelates [28] prior to experiments [5,6,53] with astonishing accuracy. For a review of DΓA, see Ref. [60]; and [122] for how to calculate T_c.

Spectrum.—We first discuss the electronic spectrum. In Fig. 2, we show the momentum dependence of the imaginary part of the Green's function at the lowest Matsubara frequency: $-\Im G(\omega_n = \pi/\beta, \mathbf{k})/\pi$ for various interactions: $U/t = 4.3, 6, 7, 8$ and fillings: $n = 0.80, 0.85, 0.90, 0.95$ for hoppings corresponding to NdPdO$_2$ ($t'/t = -0.17$, $t''/t = 0.13$). We observe that the spectrum changes from a noninteractinglike Fermi surface at weak coupling to a shape with strongly momentum-dependent damping at stronger coupling, before, finally, all spectral weight is removed. In between, we obtained a Fermi arc structure at low doping ($n_{d_{x^2-y^2}} \sim 0.90$–0.95) for $U = 7t$ and $8t$, which is a hallmark feature of cuprates.
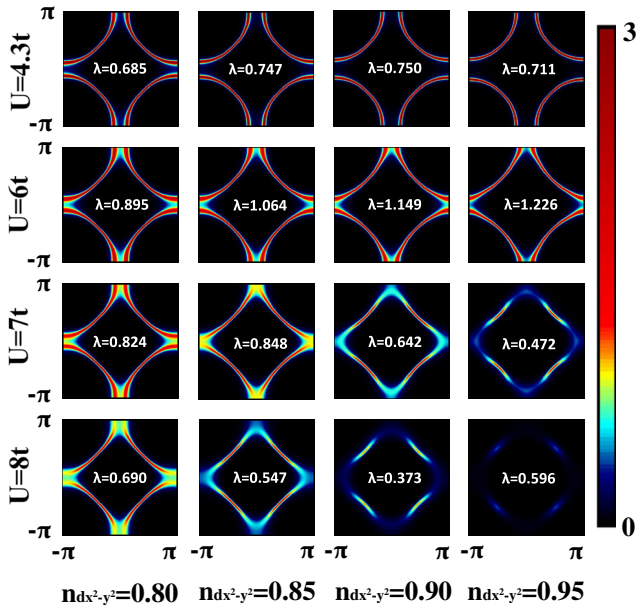

FIG. 2. DΓA Spectrum (momentum dependence of the imaginary part of the Green function $-\Im G/\pi$ at lowest Matsubara frequency) for different interactions ($U/t = 4.3, 6.0, 7.0, 8.0$) and fillings ($n = 0.80, 0.85, 0.90, 0.95$) at $T = 0.01t, t'/t = -0.17$, $t''/t = 0.13$. Corresponding d-wave superconductivity eigenvalues λ are also shown.

Even outside the pseudogap region, correlation effects change the Fermi surface structure. Specifically, they decrease the Fermi surface warping, i.e., effectively decrease t'. Such change of the spectrum for large (t', t'') region has also been observed in other theoretical studies [123–125]. These Fermi surface changes also affect the superconducting instability. While this effect (coming from the momentum dependence of $\Re\Sigma$) is minor compared with the pseudogap physics (stemming from the momentum dependence of $\Im\Sigma$), we find that such a Fermi surface flattening can enhance superconductivity, but only around the optimal conditions in parameter space; see SM [75] for a detailed discussion.

As demonstrated here, DΓA properly captures correlation-induced changes of the Fermi surface (e.g., Fermi arc in cuprates [126]) and is consistent with previous results.

Superconductivity.—Next, we discuss the superconducting instability. To do so, we calculate the eigenvalues of the linearized gap (Eliashberg) equation which is the usual procedure for evaluating the superconducting instability from the paramagnetic solution. The eigenvalue λ is a measure of the superconducting instability, and T_c is identified by λ reaching unity. While DΓA is unbiased with respect to spin, charge, and quantum critical fluctuations, we find that spin fluctuations mediate d-wave superconductivity in all cases studied.

In Fig. 3, we plot the superconducting eigenvalues against the interaction U and the filling for three tight-binding parameter sets: the simplest case ($t' = t'' = 0$), parameters for NdPdO$_2$ ($t' = -0.17t$, $t'' = 0.13t$) and NdNiO$_2$ ($t' = -0.25t$, $t'' = 0.12t$). First, we notice in all cases a strong suppression of λ around half-filling at strong coupling. This leads to a dome structure of T_c as a function of both interaction strength and filling, which is essential for optimizing superconducting materials.

Figure 3 unequivocally reveals that the origin of this suppression is too strong antiferromagnetic correlations (dark red color scale). These open a pseudogap in Fig. 2 and thus suppress the electron propagator. Even though the
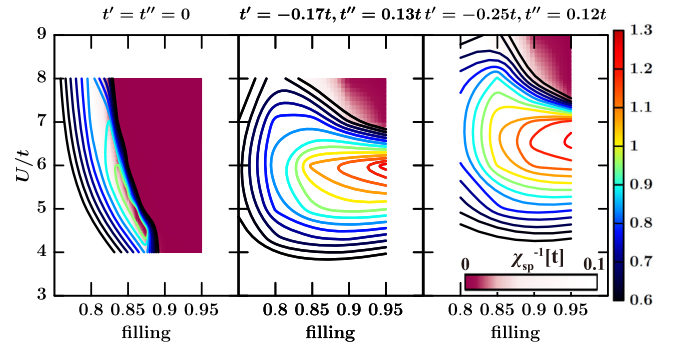

FIG. 3. Superconducting eigenvalue λ and antiferromagnetic susceptibility $\chi_{\text{sp}}(Q_{\text{max}}, \omega = 0)$ as a function of interaction U and filling at $T = 0.01t$ for the three different t', t'' given at the top of each panel.

antiferromagnetic pairing glue is huge, this eventually suppresses superconductivity.

Let us note that cluster DMFT [127] shows a similar tendency as in Fig. 3, albeit with still much higher temperatures and weaker superconducting fluctuations. The pseudogap behavior is, on the other hand, consistent with the observation that the insulating regime expands if long-range spatial fluctuations are properly included [62,128,129].

Except for the perfectly nested case ($t' = t'' = 0$) where spin fluctuations are overly strong and open a gap regardless of interaction strength, we can separate the U range into two regions: For weak couplings ($U \lesssim 5$), there is only a weak doping dependence. For strong coupling ($U \gtrsim 7$), on the other hand, a pronounced filling dependence develops, with antiferromagnetic fluctuation dominating around half-filling and suppressing λ. Optimal conditions for superconductivity in the one-band 2D square-lattice Hubbard model are realized in between these two regions. The importance of the finite Fermi surface warping was also suggested in early phenomenological material-dependence studies of cuprate superconductors [15]. The only other possibilities to significantly enhance T_c are (i) increasing t, which sets the energy scale, while keeping all parameter ratios constant, or (ii) creating a positive feedback on superconductivity from other bands including the oxygen bands in case of cuprates [17,130,131].

Figure 4 demonstrates that a dome shape of λ develops as a function of U. The optimal U slightly depends on the (t', t'') parameters. This trend can be explained by the earlier onset of the pseudogap for systems with small t', t'', due to better (antiferromagentic) nesting.

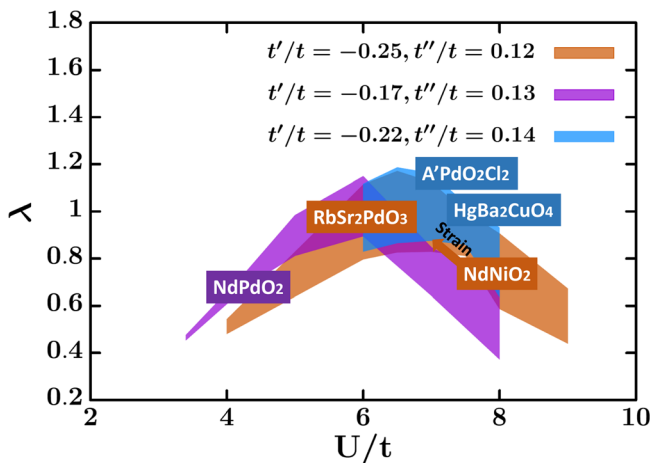In Fig. 4, we also show the points corresponding to each material from Table I. Further we include $HgBa_2CuO_4$ as a typical cuprate which has $U/t \sim 7.5t$–$8t$ [22,24,25] and almost the same t', t'' as $A_2'PdO_2Cl_2$. As mentioned in previous works [28,63], we can see that $NdNiO_2$ has an interaction that is too large and thus falls outside the area with highest T_c.

Following this insight, we can rationalize now the recent experimental achievements of realizing higher T_c's in $NdNiO_2$: both external pressure [65] and in-plane lattice compressive strains [53,132] play similar roles at reducing the in-plane lattice constant, shrinking the Ni-Ni distance, and weakening the correlation strength U/t, while increasing the magnetic exchange $4t^2/U$ [133]. Simply replacing Ni-$3d$ by Pd-$4d$ yields $NdPdO_2$ which is too weakly correlated in Fig. 4. Let us emphasize that this concerns tetragonal $NdPdO_2$ which can be stabilized in thin films. In the bulk and for thick films, there will be a substantial orthorhombic distortion, see SM [75], Section VIII. Because of the tilting of the PdO_6 octahedra, t is reduced to 304 meV. This pushes orthorhombic $NdPdO_2$ to $U/t \sim 7$, i.e., close to the optimum in Fig. 4 (average $t'/t \approx -0.25; t''/t \approx 0$). However, this enhancement of T_c/t is largely compensated by the smaller t, altogether yielding a similar T_c.

A more promising solution to increase U/t and thus T_c is to enlarge the lattice which is possible by inserting spacing layers between the PdO_2 planes. Doing so, our DFT and cRPA calculations indeed place $RbSr_2PdO_3$ and $A_2'PdO_2Cl_2$ close to the optimum.

We finally show in Fig. 5 the phase diagram for these palladate compounds, using the same approach as previously for nickelates [28]. We predict palladates to have a $T_c \gtrsim 60$ K, which touches the floor level line of cuprates and remarkably exceeds the current upper limit of nickelates, $T_c = 30$ K [53,65]. Indeed, the calculated phase diagram (superconductivity and antiferromagnetism) for
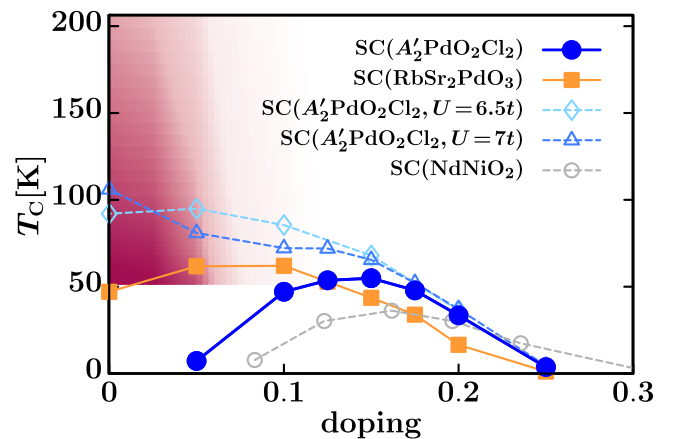
FIG. 4. Interaction U dependence of the superconducting eigenvalues λ at $T = 0.01t$ for three different t', t'' from Table I. For each U, the linewidth corresponds to the range of λ for fillings $0.80 \leq n \leq 0.90$. Materials corresponding to these models and U's are indicated.

FIG. 5. Phase diagrams for nickelates ($NdNiO_2$) and palladates ($RbSr_2PdO_3$ and $A_2'PdO_2Cl_2$). In the red region, we expect antiferromagnetism instead of superconductivity for $A_2'PdO_2Cl_2$ if there is a weak interlayer coupling because of the huge χ_{sp} (color code of χ_{sp} in DΓA as in Fig. 3).

$A_2'PdO_2Cl_2$ is quite similar to well-known cuprate phase diagrams. Furthermore, weak strain (described by $U = 6.5t, 7t$ [134], cf., Table I) would tune the material to an even higher T_c.

Conclusion and outlook.—Building on the success of DΓA to *predict* the superconducting dome in nickelates, we have performed a comprehensive survey of the Hubbard model and revealed the optimal phase-space region for unconventional superconductivity. Conditions are optimal at intermediate coupling ($U/t = 6$–7), moderate Fermi surface warping ($|t'| + |t''| \approx 0.3$–0.4), and low hole doping ($n \sim 0.90$–0.95). Combining this insight with first principles calculations, we predict palladates and nickelates grown on compressive substrates to be superconductors with a T_c comparable to cuprates.

The theoretically proposed palladates have yet to be synthesized. Palladates with a perovskitelike structure [135,136], however, have already been realized in experiment. Then, provided that a reduction process, similar to that of $NdNiO_3 \rightarrow NdNiO_2$, is possible, realizing palladates with PdO_2 layers is a promising route for high-T_c superconductors. Additionally, the possibility to engineer cuprate analogs based on $4d$ materials has been discussed based on AgF_2 [137] and silver oxides [138]. Analyzing the relation between those systems and the ones we are proposing in this Letter will offer fresh insight into the design of superconductors.

[1] J. G. Bednorz and K. A. Müller, Z. Phys. B Condens. Matter **64**, 189 (1986).

[2] D. Li, K. Lee, B. Y. Wang, M. Osada, S. Crossley, H. R. Lee, Y. Cui, Y. Hikita, and H. Y. Hwang, Nature (London) **572**, 624 (2019).

[3] L. Si, W. Xiao, J. Kaufmann, J. M. Tomczak, Y. Lu, Z. Zhong, and K. Held, Phys. Rev. Lett. **124**, 166402 (2020).

[4] P. Werner and S. Hoshino, Phys. Rev. B **101**, 041104(R) (2020).

[5] S. Zeng, C. S. Tang, X. Yin, C. Li, M. Li, Z. Huang, J. Hu, W. Liu, G. J. Omar, H. Jani, Z. S. Lim, K. Han, D. Wan, P. Yang, S. J. Pennycook, A. T. S. Wee, and A. Ariando, Phys. Rev. Lett. **125**, 147003 (2020).

[6] D. Li, B. Y. Wang, K. Lee, S. P. Harvey, M. Osada, B. H. Goodge, L. F. Kourkoutis, and H. Y. Hwang, Phys. Rev. Lett. **125**, 027001 (2020).

[7] M. Hepting, D. Li, C. J. Jia, H. Lu, E. Paris, Y. Tseng, X. Feng, M. Osada, E. Been, Y. Hikita et al., Nat. Mater. **19**, 381 (2020).

[8] Y. Nomura and R. Arita, Rep. Prog. Phys. **85**, 052501 (2022).

[9] M. Osada, B. Y. Wang, K. Lee, D. Li, and H. Y. Hwang, Phys. Rev. Mater. **4**, 121801(R) (2020).

[10] S. Zeng, C. Li, L. E. Chow, Y. Cao, Z. Zhang, C. S. Tang, X. Yin, Z. S. Lim, J. Hu, P. Yang, and A. Ariando, Sci. Adv. **8**, eabl9927 (2022).

[11] M. Osada, B. Y. Wang, B. H. Goodge, S. P. Harvey, K. Lee, D. Li, L. F. Kourkoutis, and H. Y. Hwang, Adv. Mater. **33**, 2104083 (2021).

[12] G. A. Pan et al., Nat. Mater. **21**, 160 (2022).

[13] P. W. Anderson, Science **235**, 1196 (1987).

[14] F. C. Zhang and T. M. Rice, Phys. Rev. B **37**, 3759 (1988).

[15] E. Pavarini, I. Dasgupta, T. Saha-Dasgupta, O. Jepsen, and O. K. Andersen, Phys. Rev. Lett. **87**, 047003 (2001).

[16] H. Sakakibara, H. Usui, K. Kuroki, R. Arita, and H. Aoki, Phys. Rev. Lett. **105**, 057003 (2010).

[17] C. Weber, C. Yee, K. Haule, and G. Kotliar, Europhys. Lett. **100**, 37001 (2012).

[18] H. Sakakibara, K. Suzuki, H. Usui, S. Miyao, I. Maruyama, K. Kusakabe, R. Arita, H. Aoki, and K. Kuroki, Phys. Rev. B **89**, 224505 (2014).

[19] S. W. Jang, H. Sakakibara, H. Kino, T. Kotani, K. Kuroki, and M. J. Han, Sci. Rep. **6**, 33397 (2016).

[20] S. Teranishi, K. Nishiguchi, and K. Kusakabe, J. Phys. Soc. Jpn. **87**, 114701 (2018).

[21] M. Hirayama, Y. Yamaji, T. Misawa, and M. Imada, Phys. Rev. B **98**, 134501 (2018).

[22] F. Nilsson, K. Karlsson, and F. Aryasetiawan, Phys. Rev. B **99**, 075135 (2019).

[23] H. Sakakibara and T. Kotani, Phys. Rev. B **99**, 195141 (2019).

[24] M. Hirayama, T. Misawa, T. Ohgoe, Y. Yamaji, and M. Imada, Phys. Rev. B **99**, 245155 (2019).

[25] S. Teranishi, K. Nishiguchi, and K. Kusakabe, J. Phys. Soc. Jpn. **90**, 054705 (2021).

[26] H. Watanabe, T. Shirakawa, K. Seki, H. Sakakibara, T. Kotani, H. Ikeda, and S. Yunoki, Phys. Rev. Res. **3**, 033157 (2021).

[27] J.-B. Morée, M. Hirayama, M. T. Schmid, Y. Yamaji, and M. Imada, Phys. Rev. B **106**, 235150 (2022).

[28] M. Kitatani, L. Si, O. Janson, R. Arita, Z. Zhong, and K. Held, npj Quantum Mater. **5**, 59 (2020).

[29] J. Karp, A. S. Botana, M. R. Norman, H. Park, M. Zingl, and A. Millis, Phys. Rev. X **10**, 021061 (2020).

[30] P. Worm, L. Si, M. Kitatani, R. Arita, J. M. Tomczak, and K. Held, Phys. Rev. Mater. **6**, L091801 (2022).

[31] T. Y. Xie, Z. Liu, C. Cao, Z. F. Wang, J. L. Yang, and W. Zhu, Phys. Rev. B **106**, 035111 (2022).

[32] H. Chen, A. Hampel, J. Karp, F. Lechermann, and A. J. Millis, Front. Phys. **10**, 835942 (2022).

[33] K. Held, L. Si, P. Worm, O. Janson, R. Arita, Z. Zhong, J. M. Tomczak, and M. Kitatani, Front. Phys. **9**, 810394 (2022).

[34] J. Karp, A. Hampel, and A. J. Millis, Phys. Rev. B **105**, 205131 (2022).

[35] C. Lane, R. Zhang, B. Barbiellini, R. S. Markiewicz, A. Bansil, J. Sun, and J.-X. Zhu, arXiv:2208.08375.

[36] K.-W. Lee and W. E. Pickett, Phys. Rev. B **70**, 165109 (2004).

[37] P. Adhikary, S. Bandyopadhyay, T. Das, I. Dasgupta, and T. Saha-Dasgupta, Phys. Rev. B **102**, 100501(R) (2020).

[38] Y. Wang, C.-J. Kang, H. Miao, and G. Kotliar, Phys. Rev. B **102**, 161118(R) (2020).

[39] Z. Wang, G.-M. Zhang, Y.-f. Yang, and F.-C. Zhang, Phys. Rev. B **102**, 220501(R) (2020).

[40] I. Leonov, S. L. Skornyakov, and S. Y. Savrasov, Phys. Rev. B **101**, 241108(R) (2020).

[41] S. Ryee, H. Yoon, T. J. Kim, M. Y. Jeong, and M. J. Han, Phys. Rev. B **101**, 064513 (2020).

[42] E. Been, W.-S. Lee, H. Y. Hwang, Y. Cui, J. Zaanen, T. Devereaux, B. Moritz, and C. Jia, Phys. Rev. X **11**, 011050 (2021).

[43] F. Lechermann, Phys. Rev. B **101**, 081110(R) (2020).

[44] F. Lechermann, Phys. Rev. X **10**, 041002 (2020).

[45] A. Kreisel, B. M. Andersen, A. T. Rømer, I. M. Eremin, and F. Lechermann, Phys. Rev. Lett. **129**, 077002 (2022).

[46] F. Lechermann, Phys. Rev. B **105**, 155109 (2022).

[47] X. Wan, V. Ivanov, G. Resta, I. Leonov, and S. Y. Savrasov, Phys. Rev. B **103**, 075123 (2021).

[48] M.-Y. Choi, W. E. Pickett, and K.-W. Lee, Phys. Rev. Res. **2**, 033445 (2020).

[49] F. Petocchi, V. Christiansson, F. Nilsson, F. Aryasetiawan, and P. Werner, Phys. Rev. X **10**, 041047 (2020).

[50] The rather crude classification [(1) $3d_{x^2-y^2}$ plus decoupled pockets; (2) same Fermi surface as (1) but relevance of $3d_{z^2}$ holes and coupling to the pockets; (3) additional $3d_{z^2}$ Fermi surface, possibly no pockets] neglects finer details, e.g., Hund's vs Kondo physics in (2) or the conjectured importance of $4f$ electrons [51,52].

[51] M.-Y. Choi, K.-W. Lee, and W. E. Pickett, Phys. Rev. B **101**, 020503(R) (2020).

[52] R. Zhang, C. Lane, B. Singh, J. Nokelainen, B. Barbiellini, R. S. Markiewicz, A. Bansil, and J. Sun, Commun. Phys. **4**, 118 (2021).

[53] K. Lee, B. Y. Wang, M. Osada, B. H. Goodge, T. C. Wang, Y. Lee, S. Harvey, W. J. Kim, Y. Yu, C. Murthy, S. Raghu, L. F. Kourkoutis, and H. Y. Hwang, arXiv:2203.02580.

[54] K. Higashi, M. Winder, J. Kuneš, and A. Hariki, Phys. Rev. X **11**, 041009 (2021).

[55] W. Sun, Y. Li, R. Liu, J. Yang, J. Li, S. Yan, H. Sun, W. Guo, Z. Gu, Y. Deng *et al.*, arXiv:2204.13264.

[56] P. A. Lee, N. Nagaosa, and X.-G. Wen, Rev. Mod. Phys. **78**, 17 (2006).

[57] D. J. Scalapino, Rev. Mod. Phys. **84**, 1383 (2012).

[58] E. Fradkin, S. A. Kivelson, and J. M. Tranquada, Rev. Mod. Phys. **87**, 457 (2015).

[59] B. Keimer, S. A. Kivelson, M. R. Norman, S. Uchida, and J. Zaanen, Nature (London) **518**, 179 (2015).

[60] G. Rohringer, H. Hafermann, A. Toschi, A. A. Katanin, A. E. Antipov, M. I. Katsnelson, A. I. Lichtenstein, A. N. Rubtsov, and K. Held, Rev. Mod. Phys. **90**, 025003 (2018).

[61] A. Toschi, A. A. Katanin, and K. Held, Phys. Rev. B **75**, 045118 (2007).

[62] T. Schäfer *et al.*, Phys. Rev. X **11**, 011058 (2021).

[63] H. Sakakibara, H. Usui, K. Suzuki, T. Kotani, H. Aoki, and K. Kuroki, Phys. Rev. Lett. **125**, 077003 (2020).

[64] L. Si, P. Worm, and K. Held, Crystals **12**, 656 (2022).

[65] N. N. Wang, M. W. Yang, Z. Yang, K. Y. Chen, H. Zhang, Q. H. Zhang, Z. H. Zhu, Y. Uwatoko, L. Gu, X. L. Dong, J. P. Sun, K. J. Jin, and J. G. Cheng, Nat. Commun. **13**, 4367 (2022).

[66] A. S. Botana and M. R. Norman, Phys. Rev. Mater. **2**, 104803 (2018).

[67] M. Hirayama, T. Tadano, Y. Nomura, and R. Arita, Phys. Rev. B **101**, 075107 (2020).

[68] J. Zaanen, G. A. Sawatzky, and J. W. Allen, Phys. Rev. Lett. **55**, 418 (1985).

[69] A. S. Botana and M. R. Norman, Phys. Rev. X **10**, 011024 (2020).

[70] L.-H. Hu and C. Wu, Phys. Rev. Res. **1**, 032046(R) (2019).

[71] X. Wu, D. Di Sante, T. Schwemmer, W. Hanke, H. Y. Hwang, S. Raghu, and R. Thomale, Phys. Rev. B **101**, 060504(R) (2020).

[72] Y. Nomura, M. Hirayama, T. Tadano, Y. Yoshimoto, K. Nakamura, and R. Arita, Phys. Rev. B **100**, 205138 (2019).

[73] G.-M. Zhang, Y.-f. Yang, and F.-C. Zhang, Phys. Rev. B **101**, 020501(R) (2020).

[74] M. Jiang, M. Berciu, and G. A. Sawatzky, Phys. Rev. Lett. **124**, 207004 (2020).

[75] See Supplemental Material at http://link.aps.org/supplemental/10.1103/PhysRevLett.130.166002 for details of DFT, DMFT, and DΓA calculations, as well as spectra, which includes Refs. [76–97].

[76] A. Subedi, Phys. Rev. Materials **7**, 024801 (2023).

[77] L. Bellaiche and D. Vanderbilt, Phys. Rev. B **61**, 7877 (2000).

[78] F. Tran and P. Blaha, Phys. Rev. Lett. **102**, 226401 (2009).

[79] G. H. Wannier, Phys. Rev. **52**, 191 (1937).

[80] N. Marzari and D. Vanderbilt, Phys. Rev. B **56**, 12847 (1997).

[81] I. Souza, N. Marzari, and D. Vanderbilt, Phys. Rev. B **65**, 035109 (2001).

[82] A. A. Mostofi, J. R. Yates, Y.-S. Lee, I. Souza, D. Vanderbilt, and N. Marzari, Comput. Phys. Commun. **178**, 685 (2008).

[83] V. I. Anisimov, I. V. Solovyev, M. A. Korotin, M. T. Czyżyk, and G. A. Sawatzky, Phys. Rev. B **48**, 16929 (1993).

[84] E. Gull, A. J. Millis, A. I. Lichtenstein, A. N. Rubtsov, M. Troyer, and P. Werner, Rev. Mod. Phys. **83**, 349 (2011).

[85] J. Kaufmann and K. Held, arXiv:2105.11211.

[86] J. E. Gubernatis, M. Jarrell, R. N. Silver, and D. S. Sivia, Phys. Rev. B **44**, 6011 (1991).

[87] A. W. Sandvik, Phys. Rev. B **57**, 10287 (1998).

[88] T. Schäfer, A. A. Katanin, M. Kitatani, A. Toschi, and K. Held, Phys. Rev. Lett. **122**, 227201 (2019).

[89] P. C. Hohenberg, Phys. Rev. **158**, 383 (1967).

[90] N. D. Mermin and H. Wagner, Phys. Rev. Lett. **17**, 1133 (1966).

[91] C. Eckhardt, K. Hummer, and G. Kresse, Phys. Rev. B **89**, 165201 (2014).

[92] https://www.mail-archive.com/wien@zeus.theochem.tuwien.ac.at/msg11726.html.

[93] A. Togo and I. Tanaka, Scr. Mater. **108**, 1 (2015).

[94] G. Kresse and J. Furthmüller, Comput. Mater. Sci. **6**, 15 (1996).

[95] G. Kresse and J. Furthmüller, Phys. Rev. B **54**, 11169 (1996).

[96] F. Bernardini, A. Bosin, and A. Cano, Phys. Rev. Mater. **6**, 044807 (2022).

[97] C. Xia, J. Wu, Y. Chen, and H. Chen, Phys. Rev. B **105**, 115134 (2022).

[98] P. Blaha, K. Schwarz, F. Tran, R. Laskowski, G. K. H. Madsen, and L. D. Marks, J. Chem. Phys. **152**, 074101 (2020).

[99] J. P. Perdew, K. Burke, and M. Ernzerhof, Phys. Rev. Lett. **77**, 3865 (1996).

[100] J. P. Perdew, A. Ruzsinszky, G. I. Csonka, O. A. Vydrov, G. E. Scuseria, L. A. Constantin, X. Zhou, and K. Burke, Phys. Rev. Lett. **100**, 136406 (2008).

[101] J. Kuneš, R. Arita, P. Wissgott, A. Toschi, H. Ikeda, and K. Held, Comput. Phys. Commun. **181**, 1888 (2010).

[102] N. Marzari, A. A. Mostofi, J. R. Yates, I. Souza, and D. Vanderbilt, Rev. Mod. Phys. **84**, 1419 (2012).

[103] We employed a slightly different version of cRPA calculations [104] than previously [28], to better capture material differences. While we still enhance U to mimic the frequency dependence and other over-screening effects, the enhancement used here is slightly smaller than in Ref. [28].

[104] T. Miyake, F. Aryasetiawan, and M. Imada, Phys. Rev. B **80**, 155134 (2009).

[105] Single orbital parameters for two palladates: $RbSr_2PdO_3$ and $A'_2PdO_2Cl_2$ are already derived in the preceding study [24]. We obtained consistent results in our calculation and used them for further DMFT and DΓA calculations.

[106] K. Held, A. Katanin, and A. Toschi, Prog. Theor. Phys. **176**, 117 (2008).

[107] A. A. Katanin, A. Toschi, and K. Held, Phys. Rev. B **80**, 075104 (2009).

[108] H. Kusunose, J. Phys. Soc. Jpn. **75**, 054713 (2006).

[109] W. Metzner and D. Vollhardt, Phys. Rev. Lett. **62**, 324 (1989).

[110] A. Georges, G. Kotliar, W. Krauth, and M. J. Rozenberg, Rev. Mod. Phys. **68**, 13 (1996).

[111] G. Kotliar and D. Vollhardt, Phys. Today **57**, No. 3, 53 (2004).

[112] J. Otsuki, H. Hafermann, and A. I. Lichtenstein, Phys. Rev. B **90**, 235132 (2014).

[113] M. Kitatani, N. Tsuji, and H. Aoki, Phys. Rev. B **92**, 085104 (2015).

[114] M. Kitatani, N. Tsuji, and H. Aoki, Phys. Rev. B **95**, 075109 (2017).

[115] J. Vučičević, T. Ayral, and O. Parcollet, Phys. Rev. B **96**, 104504 (2017).

[116] D. Vilardi, C. Taranto, and W. Metzner, Phys. Rev. B **99**, 104501 (2019).

[117] S. Sayyad, E. W. Huang, M. Kitatani, M.-S. Vaezi, Z. Nussinov, A. Vaezi, and H. Aoki, Phys. Rev. B **101**, 014501 (2020).

[118] G. V. Astretsov, G. Rohringer, and A. N. Rubtsov, Phys. Rev. B **101**, 075109 (2020).

[119] M. Kitatani, Y. Nomura, M. Hirayama, and R. Arita, arXiv:2205.00239.

[120] M. Wallerberger, A. Hausoel, P. Gunacker, A. Kowalski, N. Parragh, F. Goth, K. Held, and G. Sangiovanni, Comput. Phys. Commun. **235**, 388 (2019).

[121] M. Kitatani, T. Schäfer, H. Aoki, and K. Held, Phys. Rev. B **99**, 041115(R) (2019).

[122] M. Kitatani, R. Arita, T. Schäfer, and K. Held, JPhys. Mater. **5**, 034005 (2022).

[123] W. Wu, M. S. Scheurer, S. Chatterjee, S. Sachdev, A. Georges, and M. Ferrero, Phys. Rev. X **8**, 021048 (2018).

[124] R. Rossi, F. Šimkovic, and M. Ferrero, Europhys. Lett. **132**, 11001 (2020).

[125] M. Klett, P. Hansmann, and T. Schäfer, Front. Phys. **10**, 834682 (2022).

[126] T. Yoshida, X. J. Zhou, K. Tanaka, W. L. Yang, Z. Hussain, Z.-X. Shen, A. Fujimori, S. Sahrakorpi, M. Lindroos, R. S. Markiewicz, A. Bansil, S. Komiya, Y. Ando, H. Eisaki, T. Kakeshita, and S. Uchida, Phys. Rev. B **74**, 224510 (2006).

[127] X. Chen, J. P. F. LeBlanc, and E. Gull, Phys. Rev. Lett. **115**, 116402 (2015).

[128] T. Schäfer, F. Geles, D. Rost, G. Rohringer, E. Arrigoni, K. Held, N. Blümer, M. Aichhorn, and A. Toschi, Phys. Rev. B **91**, 125109 (2015).

[129] F. Šimkovic, J. P. F. LeBlanc, A. J. Kim, Y. Deng, N. V. Prokof'ev, B. V. Svistunov, and E. Kozik, Phys. Rev. Lett. **124**, 017003 (2020).

[130] D. Rybicki, M. Jurkutat, S. Reichardt, C. Kapusta, and J. Haase, Nat. Commun. **7**, 11413 (2016).

[131] N. Kowalski, S. S. Dash, P. Sémon, D. Sénéchal, and A.-M. Tremblay, Proc. Natl. Acad. Sci. U.S.A. **118**, e2106476118 (2021).

[132] X. Ren, Q. Gao, Y. Zhao, H. Luo, X. Zhou, and Z. Zhu, arXiv:2109.05761.

[133] O. Ivashko, M. Horio, W. Wan, N. B. Christensen, D. E. McNally, E. Paris, Y. Tseng, N. E. Shaik, H. M. Rønnow, H. I. Wei, C. Adamo, C. Lichtensteiger, M. Gibert, M. R. Beasley, K. M. Shen, J. M. Tomczak, T. Schmitt, and J. Chang, Nat. Commun. **10**, 786 (2019).

[134] For drawing the $U = 6.5t$ phase diagram, we averaged the −1.5%, −3.0%-strain result from Table I.

[135] S.-J. Kim, S. Lemaux, G. Demazeau, J.-Y. Kim, and J.-H. Choy, J. Mater. Chem. **12**, 995 (2002).

[136] S.-J. Kim, S. Lemaux, G. Demazeau, J.-Y. Kim, and J.-H. Choy, J. Am. Chem. Soc. **123**, 10413 (2001).

[137] J. Gawraczyński, D. Kurzydłowski, R. A. Ewings, S. Bandaru, W. Gadomski, Z. Mazej, G. Ruani, I. Bergenti, T. Jaroń, A. Ozarowski et al., Proc. Natl. Acad. Sci. U.S.A. **116**, 1495 (2019).

[138] M. Hirayama, M. Thobias Schmid, T. Tadano, T. Misawa, and M. Imada, arXiv:2207.12595.